Co-published by
Institute of Fluid-Flow Machinery
Polish Academy of Sciences
Committee on Thermodynamics and Combustion
Polish Academy of Sciences

http://www.imp.gda.pl/archives-of-thermodynamics/

CFD analysis of the effect of bed geometry on H_2O adsorption and desorption efficiency

Szymon Janusz[a,b*], Marcin Borcuch[b], Piotr Cyklis[a]

[a]Cracow University of Technology, Jana Pawla II 37, 31-864 Kraków, Poland
[b]M.A.S. Sp z o.o., Research and Development Department, Składowa 34, 27-200 Starachowice, Poland
*Corresponding author email: szymon.janusz@doktorant.pk.edu.pl

Received: 29.01.2024; revised: 22.05.2024; accepted: 12.06.2024

Abstract

The article presents a comprehensive computational fluid dynamics analysis of the adsorption and desorption cycles in adsorption refrigeration systems, focusing on the impact of the adsorbent bed geometry. The entire adsorption/desorption cycle has been modeled, allowing for the observation of events during the transitional period between processes and how these influence their progression. This approach is a novelty in the field. The developed numerical model was verified against experimental data available in the literature, demonstrating excellent convergence with the experiment, with a deviation not exceeding 2%. The study illustrates how the geometrical parameters such as height and length of the bed affect the efficiency of the adsorption and desorption processes, emphasizing the importance of bed geometry in the adsorption of heat and mass exchangers in energy and adsorbate transfer. The research findings provide valuable insights for designing more efficient cooling devices using adsorption technology, highlighting the role of bed geometry in optimizing these systems. Modeling the entire adsorption/desorption cycle is a novelty and allows for the observation of what happens during the transitional period between processes and how this influences their progression.

Keywords: Heat transfer; Adsorption; Computational fluid dynamics; Mass transfer; Refrigeration devices

Vol. 45(2024), No. 3, 39–47; doi: 10.24425/ather.2024.151214

Cite this manuscript as: Janusz, S., Borcuch, M., & Cyklis P. (2024). CFD analysis of the effect of bed geometry on H_2O adsorption and desorption efficiency. *Archives of Thermodynamics*, 45(3), 39−47.

1. Introduction

The ongoing pursuit of energy-efficient and environmentally sustainable cooling technologies has catalyzed the development of several alternatives to conventional vapour compression systems. A notable breakthrough in this domain is adsorption cooling technology, which harnesses the principles of adsorption and desorption of a refrigerant onto an adsorbent material. This approach has garnered significant attention for its ability to effectively utilize waste heat and significantly reduce greenhouse gas emissions, marking a substantial leap in eco-conscious cooling solutions. Due to their innovative operating mechanism, adsorption cooling systems present a promising prospect, yet they are continuously subject to enhancements and development. These systems are characterized by a relatively modest Coefficient of Performance (COP) and considerable size, factors which currently limit their competitiveness in the broader market. The challenge in optimizing these devices lies in the complexity and cost associated with adjusting various interdependent parameters, which intricately affect the device's performance. In this

Nomenclature

a_{sv} – interfacial area density, m^{-1}
D_p – diameter of the bed particles, m
h_{sv} – heat transfer coefficient in porous bed, W/(m^{2}K)
k – thermal conductivity of the medium W/(m K)
$\dot{m}$ – mass flow rate
Nu – Nusselt number
P – pressure, Pa
T – temperature, K

Greek symbols

ε – porosity of the medium
τ – time, s

Subscripts and Superscripts

a – average
A – absolute
f – fluid
s – surface
t – total
v – vapour

Abbreviations and Acronyms

CFD – computational fluid dynamics
COP – coefficient of performance
PISO – pressure implicit with splitting of operators
UDF – user defined function

context, Computational Fluid Dynamics (CFD) emerges as an invaluable tool for advancing our understanding and enhancing the efficiency of these systems.

In paper [1], numerical simulations of a real-scale adsorption chiller, including a sorption chamber with a bed, condenser, and evaporator, were conducted. The results were verified against experimental setups, showing high consistency with deviations not exceeding 2%. This demonstrates the legitimacy of the usage of numerical models for optimizing adsorption chillers. In the study [2], the authors present a methodology for conducting numerical simulations of adsorption and desorption processes in adsorbent beds, utilizing CFD techniques. The research focuses on analyzing the impact of various factors, such as the cooling water temperature and cycle duration, on the performance of adsorption chillers. In another work, researchers employed CFD simulations to examine the influence of silica gel grain size on the efficiency of the adsorption process, thereby identifying optimal grain dimensions for maximal operational effectiveness [3]. Similarly, investigations into the spatial distribution of porosity gradients have illuminated their critical role in enhancing the cooling performance of adsorption-based systems. Employing CFD simulations, researchers have validated the significance of directional porosity distribution in improving cooling efficiency [4]. Analysis of various adsorbent-adsorbate combinations has revealed superior performance in coated beds versus densely packed ones [5]. The impact of the temperature of the cooling and heating medium on the sorbent bed was described in the paper [6]. Despite these advancements, there remains a need to fully comprehend the impact of adsorbent bed geometry on the performance of adsorption chillers, particularly in light of novel adsorbent materials and innovative bed configurations that have emerged in recent years. In the study [7], the authors designed and constructed a fin of the heat exchanger, increasing the efficiency of the adsorption process. The improvement was not significant due to the limitations of 3D printing; however, this remains an interesting direction for future research. In the paper [8] the authors proposed using a modified plate heat exchanger in adsorption devices. Both experimental and numerical results showed a 310% increase in differential water absorption after 300 seconds from the start of adsorption compared to standard adsorbers with aluminium fins.

One of the most critical components in adsorption chillers is the adsorbent bed. The design and structural geometry of the bed significantly influences heat and mass transfer processes, thus directly impacts the overall efficiency of the adsorption chiller. Extensive research has been undertaken to explore the effect of bed geometry on the efficiency of the adsorption process. Studies have shown, that a thin, flatbed geometry outperforms a cylindrical configuration in analyzed conditions [9]. Additionally, research findings suggest that a compact bed layout with a high surface-to-volume ratio can enhance chiller efficiency [5]. In the study [10], the authors conducted research on optimizing the adsorbent bed. It focuses on optimal geometric parameters and the impact of metal additives. Numerical simulations were used, analyzing the adsorbent bed with metals and silica gel/water pair. The study reveals that adding aluminium particles significantly enhances cooling performance, showing a 300% efficiency increase with the addition of aluminium particles. In a different study [11], adsorbent beds with vacuum tubes and fins were experimentally tested. It was found that beds with more fins shortened the cooling time but lengthened the preheating and desorption times. The system's optimal performance was achieved with four fins, and additional fin enhancement did not further improve the efficiency of the adsorption cooling system. This suggests that each bed geometry has an optimal number of fins, and more fins do not always equate to better performance. In the paper [12], the impact of fin thickness and height, as well as plate type, on the efficiency of an adsorbent bed were investigated. The study revealed that decreasing fin thickness could enhance water adsorption by up to 8%, and reducing fin height from 30mm to 20mm could increase adsorption by up to 17%. Additionally, the type of plate used was found to be significant, with a copper plate improving water adsorption by up to 9% compared to an aluminium plate. Using CFD simulations, the importance of the Z-direction in porosity distribution and its significant impact on cooling efficiency have been validated [13]. Furthermore, investigations into different adsorbent-adsorbate pairings have demonstrated improved performance in coated beds compared to packed beds [14].

Despite these research advancements, a comprehensive understanding of how the geometry of the adsorbent bed influences the performance of adsorption chillers remains crucial. The efficiency of adsorption in cooling systems is a complex measure of how effectively the system utilizes the adsorption-desorption cycle to generate a cooling effect. This process is more complicated than a simple relationship between the amount of water

vapour adsorbed by the adsorbent and the efficiency of cooling. Key aspects, such as adsorption capacity and rate, are significant but represent only a part of the equation. In thermodynamic terms, the timing of the cycle involving adsorption and desorption is fundamental. A cycle that is too short may not provide sufficient regeneration of the adsorbent, while a cycle that is too long can decrease overall operational efficiency. Therefore, not only the intensity of vapour adsorption is important, but also the optimization of the cycle time based on specific conditions and system requirements. Furthermore, the geometry and size of the device are crucial. The time required to switch between the adsorption and desorption phases and the stabilization of the process can impact efficiency to the extent that lengthening the cycle becomes more advantageous. In this context, optimizing the adsorbent bed and heat exchanger geometries is particularly important. Efficient and controlled heat transfer is essential for maximizing the cycle's efficiency. This research aims to demonstrate specific correlations between the geometry of the adsorbent bed and the adsorption process, ultimately influencing the efficiency of adsorption-based cooling devices.

2. Methods

The sample analyzed is a representative part of a plate heat exchanger used in adsorption refrigeration devices. The model consists of a wall simulating the heat exchanging surface, where a convective boundary condition is established with a heat transfer coefficient of 600 W/(m²K), consistent with the experimental setup described in the literature [15], and a temperature of 303 K, corresponding to the cooling water temperature for the adsorbent bed. On this wall, a layer of silica gel, serving as an adsorbent in a water vapour atmosphere (adsorbate), is applied. The silica gel sample is enclosed in an aluminium frame, which restricts vapour flow in one direction, and an adiabatic boundary condition is applied to it. This inflow is modelled as a pressure boundary condition with a P_A = 2000 Pa and an incoming water vapour temperature T_v = 290.15 K. The operating pressure within the model is set to 0 Pa, and the model features only a vapour inlet with no outlet. The study involved simulating the adsorption process in beds of various dimensions, where the base dimensions are set as 100×80×6 mm (Fig. 1).

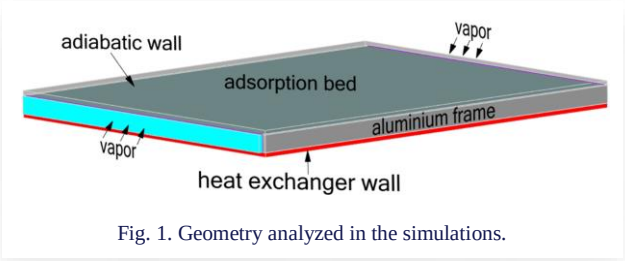

Fig. 1. Geometry analyzed in the simulations.

The model was discretized using the SWEEP method. Prepared geometry enabled the creation of a well-organized structural mesh across the entire model. In order to perform grid convergence tests, three grids differing by a factor of 1.5 in their characteristic dimension were generated. Each grid was characterized by a minimum orthogonal quality equal to 1. Detailed information about the prepared grids is gathered in Table 1. Differences in the values of adsorbed vapour and average temperature in the adsorption bed between the results obtained for the individual grids result from the applied global grid size. Considering the very small differences in values between the fine and medium grids, it was decided to use the medium density grid (Fig. 2) for further work, as a compromise between computational cost and solution accuracy.

Table 1. Parameters of meshes used in the grid convergence study.

Mesh	Characteristic dimension of mesh elements [mm]	Total number of mesh elements	Orthogonal quality	Average bed temperature [K]	Uptake [kg/kg]
Coarse	0.7	125350	1	315.255	0.1209
Medium	0.5	207360	1	314.925	0.1212
Fine	0.3	613452	1	314.903	0.1212

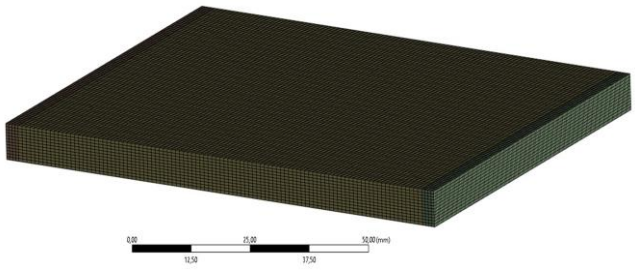

Fig. 2. Numerical mesh generated.

In this study, a CFD modelling approach for the adsorption process as described in paper [2] was adopted. The calculations were performed using Ansys Fluent software. For the modeling of the porous volume, the equilibrium model was replaced with a non-equilibrium model, which is defined by two parameters: Interfacial Area Density and Heat Transfer Coefficient in ANSYS Fluent software.

Interfacial Area Density a_{sv} is a parameter used in multiphase flow simulations within porous media. It measures the area of the interface between different phases (e.g. liquid and solid) per unit volume of the porous material. This parameter is crucial for predicting phenomena such as mass and heat transfer accurately

$$a_{sv} = \frac{6(1-\varepsilon_t)}{D_p}. \quad (1)$$

Heat transfer coefficient h_{sf} in a porous medium is a parameter that quantifies the efficiency of heat transfer between the fluid and the solid structure within the porous material

$$\frac{1}{h_{sf}} = \frac{D_p}{k_f \mathrm{Nu}} + \frac{D_p}{10k_f}. \quad (2)$$

The simulation was conducted under transient conditions. It was assumed that the flow of water vapour is laminar. The Green-Gauss node based gradient computation scheme, along with the QUICK momentum discretization scheme, were employed. A pressure-based solver utilizing the PISO scheme was used.

The model was verified against an experiment available in the literature [15]. The experiment was conducted on a specially constructed experimental setup that simulated the operation of an adsorption refrigeration device. The sorption capacity of a silica gel sample was analyzed under various temperatures of the cooling/heating medium. The maximum deviation between the numerical simulation and experimental data did not exceed 2% (Fig. 3), indicating very good convergence of the developed numerical model.

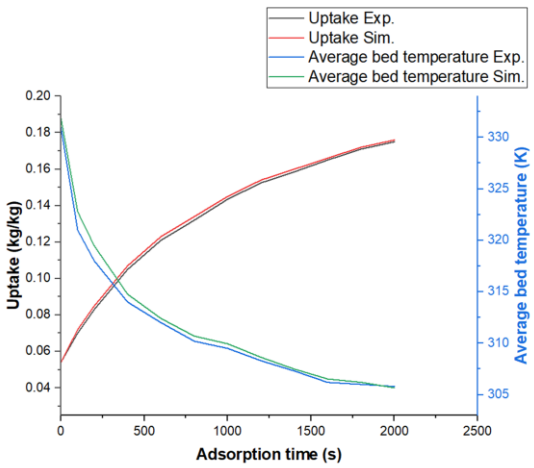

Fig. 3. Comparison of experimental and numerical results: average bed temperature and the amount of adsorbed water vapour in the bed.

For further simulations, initial conditions were set: T = 303.15 K, P = 2000 Pa, and H_2O uptake 0 g/g. Each cycle consisted of two stages: adsorption, where the sorption bed was cooled, and regeneration (desorption), where the bed was heated. As the adsorption process ends and desorption begins, the function of the heat exchanger plate switches from cooling to heating. Consequently, expressions for the cyclic change of the boundary condition from 303.15 K to 353.15 K were introduced. During desorption, as vapour is released from the bed, the boundary condition changes from a pressure inlet to a pressure outlet. For this purpose, a UDF (user defined function) was prepared and implemented to monitor the P in the adsorption bed. This function calculates and returns the P_a in a specified area, allowing observation of P changes over time. Moreover, it defines pressure boundary conditions that trigger the change in boundary conditions. Iterative calculations, consisting of 3000 time steps (5 full cycles of 600 seconds each) were performed. Each step lasted one second and could include up to 500 iterations until a reduction of normalized residuals by four orders of magnitude was achieved. However, it's important to note that sudden changes in temperature and pressure may lead to discrepancies in simulation results. Therefore, during transitions from adsorption to desorption and vice versa, a reduction in the time step of the simulation from 1 s to 0.005 s for the next 5 seconds was applied. As a result, convergence was achieved at the level of $4x10^{-5}$ for all residuals. Additionally, the vapour velocity at the inlet, temperature in the adsorption bed, and the amount of water vapour adsorbed by the bed were monitored.

Within the scope of this study, the adsorption process was simulated for beds of various dimensions. The base dimensions of the bed were 100×80×6 mm. The first step involved examining the effect of increasing the bed height to 6 mm and 9 mm (Fig. 4a). Subsequently, an analysis was conducted on changing the bed length to 50 mm and 150 mm (Fig. 4b).

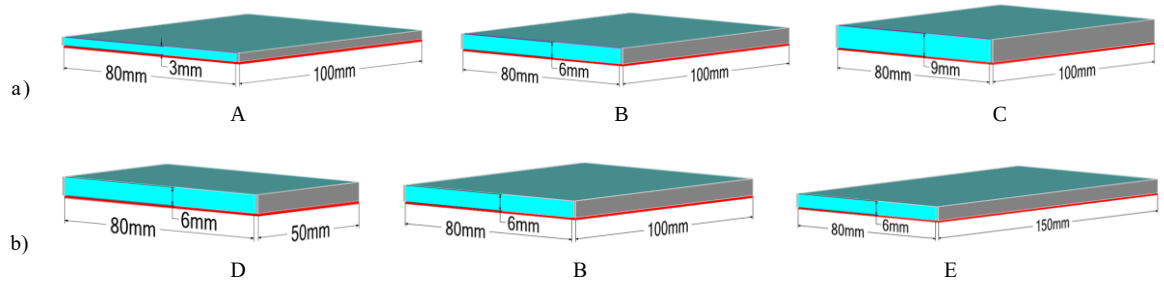

Compilation of silica gel mass depending on the geometry of the bed.

Geometry	A	B	C	D	E
Mass of silica gel [kg]	0.01776	0.03552	0.05328	0.00888	0.02664

Fig. 4. Dimensions of the simulated samples: a) various heights of the adsorbent bed, b) various lengths of the adsorbent bed.

3. Results

Due to significant differences in saturation values between various stages of the simulation, different scales were applied to better illustrate the processes occurring within the bed (Figs. 5a, 5b). Graphical distribution of the amount of vapour adsorbed by the sorption bed (Figs. 5a, 6a,7a) at τ = 300 s, corresponding to the end of the adsorption process in the first cycle, and at 600 s, corresponding to the end of the desorption process in the first cycle. Similarly, the amount of vapour adsorbed after 2700 s (Figs. 5b, 6b, 7b) – marking the end of the adsorption process in the last cycle, and at 3000 s - marking the end of desorption in the last analyzed cycle. The graphical distributions (Figs. 5, 6, 7) indicate that for all analyzed geometries, both adsorption and desorption processes occur most efficiently near the wall

heated/cooled by the heat exchanger and at the water vapour inlet surface, highlighting the significance of *T* on the adsorption/desorption processes. It is observed that the saturation of the bed with water vapour increases with each process cycle, suggesting that adsorption and desorption do not occur uniformly. The ratio of the amount of adsorbed vapour to the size of the bed is highest for the bed with the smallest height and lowest for the tallest bed, confirming the importance of the distance from the centre of the bed to the heat exchange surface.

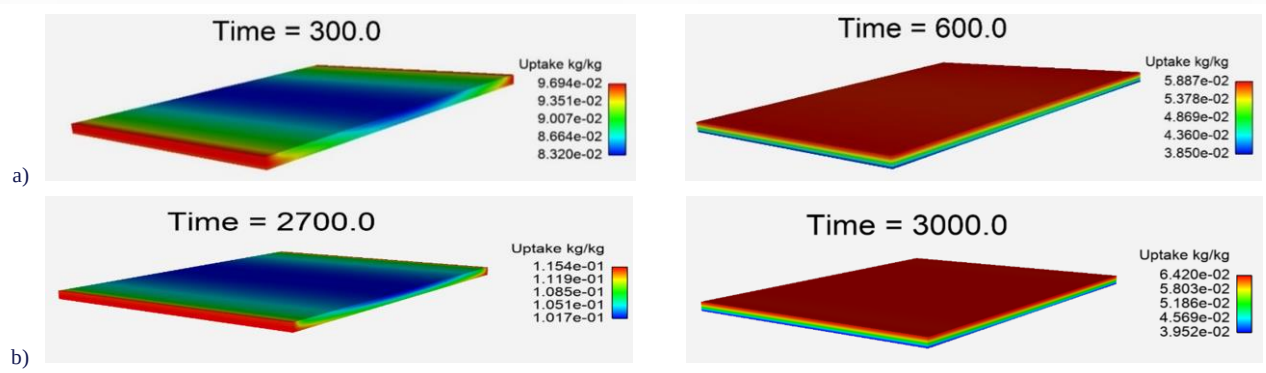

Fig. 5. Distribution of the amount of vapour adsorbed by the sorption bed with dimensions of 100×80×3 mm (A) after adsorption and desorption process: a) in the first cycle of the process b) in the last cycle of the process.

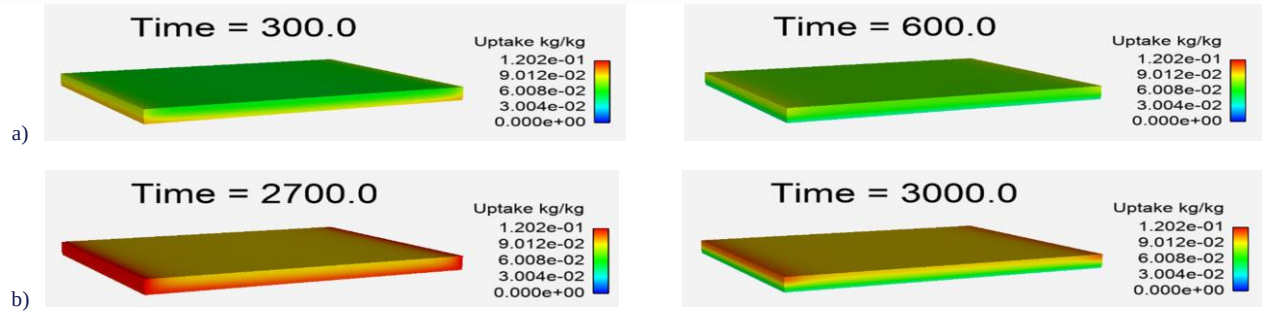

Fig. 6. Distribution of the amount of vapour adsorbed by the sorption bed with dimensions of 100×80×3 mm (B) after adsorption and desorption process a) in the first cycle of the process b) in the last cycle of the process.

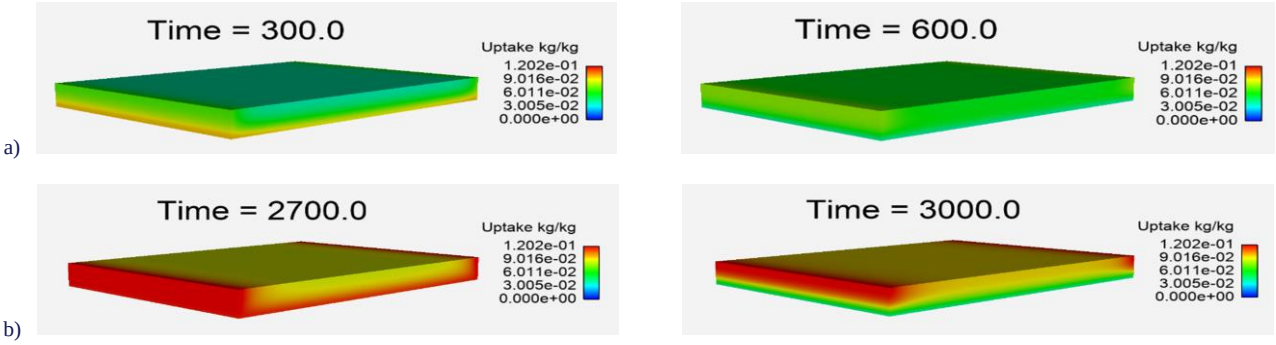

Fig. 7. Distribution of the amount of vapour adsorbed by the sorption bed with dimensions of 100×80×3 mm (C) after adsorption and desorption process a) in the first cycle of the process b) in the last cycle of the process.

The amount of vapour adsorbed was analyzed for beds of varying heights (Fig. 8). The stabilization of the process in successive cycles was quickest for the bed with the lowest height and slowest for the bed with the greatest height. For beds B and C heights, similar saturation values after the desorption process were observed in the initial cycles, which increased with subsequent cycles. According to the analysis of graphical distributions, the most vapour relative to the amount of adsorbent material in each cycle was adsorbed by bed A, stabilizing at 0.132 kg/kg. The least amount of vapour was adsorbed in bed C, stabilizing at 0.111 g/g which represents a difference of approximately 20%. In the adsorption bed A, vapour desorbed to a level of 0.041 kg/kg, whereas in the bed C, it desorbed to 0.074 kg/kg, constituting a difference of about 45%. The dynamics of the process varied depending on the height of the bed. Adsorption was most intense for the bed A and least intense for the bed C. This can be attributed to the fact that cooling of the bed during the adsorption process significantly influences its progression, and

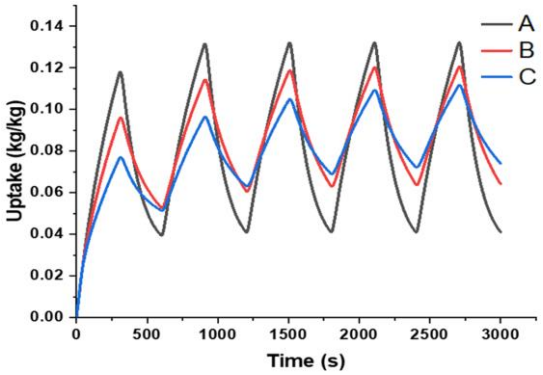

Fig. 8. Comparison of the amount of water vapour adsorbed for different bed heights.

heat exchange within the bed itself is inefficient.

A comparison of T_a in sorption beds with different geometries during the processes of adsorption and desorption was examined (Fig. 9).

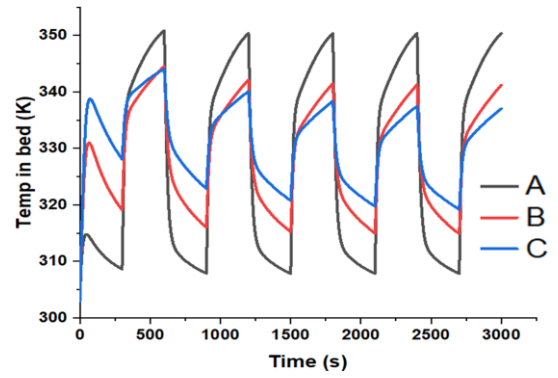

Fig. 9. Comparison of the T_a in sorption beds for different bed heights.

The bed A reaches an T_a at the end of each cycle stage that is closest to the T occurring in the heat exchanger, 308 K after adsorption and 350 K after desorption. This facilitates the most efficient adsorption/desorption process and has a direct impact on greater control over the process. In the case of the bed C, the T_a in the bed deviates more significantly from the T of the cooling/heating medium, recording 320 K at the end of the adsorption process and 337 K after desorption, which affects the amount of vapour adsorbed.

The mass flow of water vapour adsorbed by the sorption bed is illustrated (Fig. 10). Negative values indicate that vapour is being released and evaporates from the sorption bed. During the first cycle, where the saturation of each bed with water vapour was 0 kg/kg, the most intense $\dot{m}_v$ occurred in the bed C, reaching 1.13×10^{-2} g/s, which directly depended on the volume of the sorbent. In subsequent cycles, as conditions stabilize, the differences in $\dot{m}_v$ decrease, in the last cycle for beds B and C, they are very similar, with the initial adsorption rate being approximately 3.02×10^{-3} g/s.

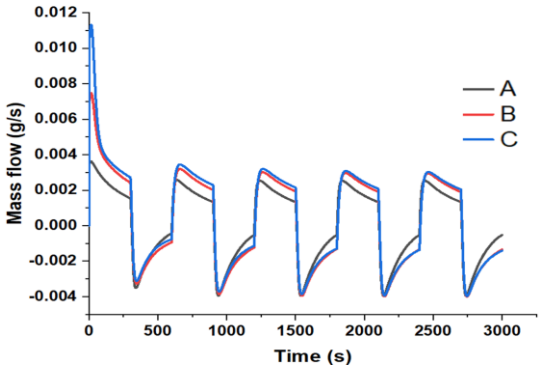

Fig. 10. Results of solar collector field simulation – hourly heating output.

Subsequently, an analysis was conducted to assess the impact of bed length on the adsorption process. An aluminium frame restricted the steam inlet and directed the steam along the length of the bed. Beds with dimensions of 50×80×6 mm (D), 100×80×6 mm (B), and 150×80× 6 mm (E) were analyzed (Fig. 5b).

Similarly to Figs. 5–7, Figs. 11–13 illustrate the graphical distribution of the amount of vapour adsorbed by the sorption bed at times corresponding to the end of the adsorption process in the first and last cycles, as well as at times corresponding to the end of the desorption process in the first and last cycles. The graphical distributions indicate similar dependencies as observed in the earlier analysis. The most efficient adsorption and desorption processes occur near the wall heated/cooled by the heat exchanger and at the surface where water vapour enters.

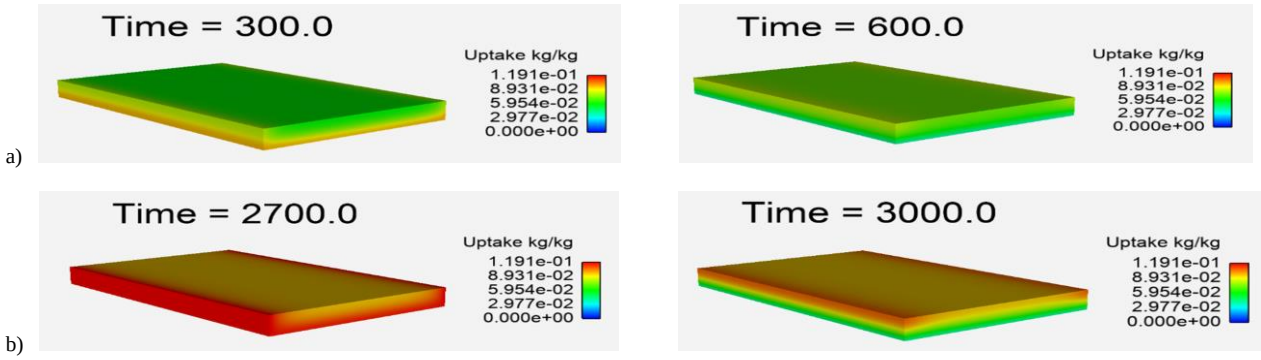

Fig. 11. Distribution of the amount of vapour adsorbed by the sorption bed with dimensions of 50×80×6 mm (D) after adsorption and desorption process a) in the first cycle of the process, b) in the last cycle of the process.

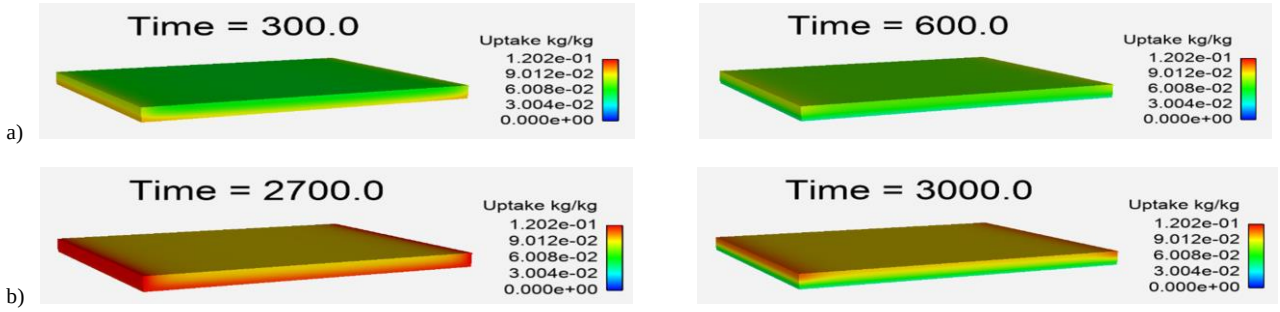

Fig. 12. Distribution of the amount of vapour adsorbed by the sorption bed with dimensions of 100×80×6 mm (B) after adsorption and desorption process a) in the first cycle of the process, b) in the last cycle of the process.

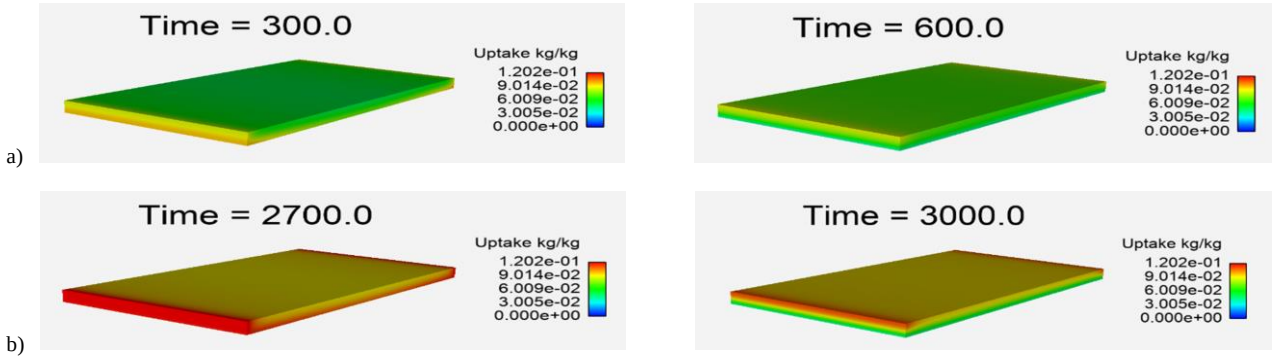

Fig. 13. Distribution of the amount of vapour adsorbed by the sorption bed with dimensions of 150×80×6 mm (E) after adsorption and desorption process a) in the first cycle of the process b) in the last cycle of the process.

The amount of vapour adsorbed for beds of varying lengths was analyzed (Fig. 14). The saturation value for the shortest bed D in the fifth cycle at the end of adsorption was 0.123 kg/kg, while for the longest bed E it was 0.117 kg/kg. In the case of desorption at the end of the process, the saturation for a bed D was 0.0645 kg/kg, and for E it was 0.0641 kg/kg. The length of the bed was more significant for the adsorption process than for desorption. It is observed that the impact of bed length on the process is less significant compared to the previously discussed bed height. It is noteworthy that as the duration of a single cycle increases, the differences in saturation also increase. This is attributed to the fact that the more saturated the bed is, the greater the resistance it poses to the flow of adsorbed vapour. Such a connection can be beneficial in selecting the optimal cycle time for a heat exchanger of a specific size.

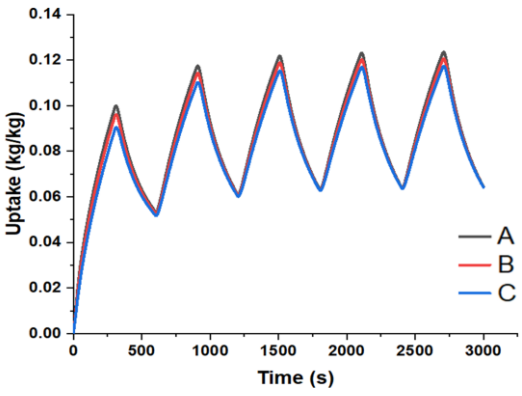

Fig. 14. Comparison of the amount of water vapour adsorbed for different lengths of the bed.

Similarly to the case of vapour adsorbed by the bed, the T_a within the sorption bed shows little variation for different lengths of the adsorption bed (Fig. 15). T_a stabilizes by the second cycle, reaching 314 K at the end of adsorption and 341 K at the end of desorption. These similar T_a in the sorption bed may explain the comparable dynamics of the adsorption and desorption processes discussed earlier.

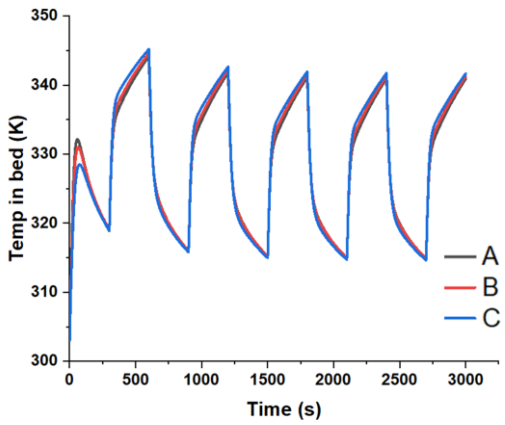

Fig. 15. Comparison of the average temperature in sorption beds for different lengths of the bed.

The mass flow of water vapour adsorbed by the bed for different lengths of the bed is illustrated (Fig. 16). Similar to the analysis of the height of the sorption bed, during the first cycle, where the saturation of each bed with water vapour was 0 kg/kg, the most intense $\dot{m}_v$ occurred. The $\dot{m}_v$ stabilizes by the second

cycle for each of the analyzed cases. For the bed E, $\dot{m}_v$ is highest, registering 4.094×10^{-3} g/s at the beginning of the adsorption stage and -5.554×10^{-3} g/s at the end of desorption. The lowest $\dot{m}_v$ was in the bed D, with values of 1.559×10^{-3} g/s at the beginning of adsorption and -2.112×10^{-3} g/s at the beginning of desorption. In the case of varying bed lengths, a clear difference in $\dot{m}_v$ between the beds is observed for all cases. It can be concluded that increasing the length of the bed has a direct impact on enhancing the suction force of water vapour.

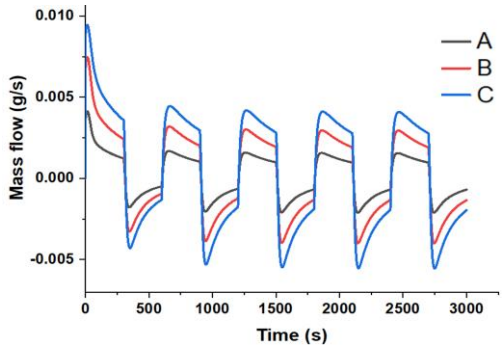

Fig. 16. Comparison of the mass flow of water vapour at the inlet to sorption beds for different lengths of the bed.

The saturation of water vapour in the adsorbent bed during the last, fifth cycle of simulation post-adsorption and desorption processes for all analyzed bed geometries was compiled (Fig. 17). Additionally, the mass of water vapour adsorbed by these beds is presented. The highest saturation, indicating the greatest sorption capacity, was exhibited by bed A, characterized by the shortest distance from the heat source to the centre of the bed, measuring 3 mm. Despite having a sorbent material volume three times smaller than bed C, bed A adsorbed only 20% less vapour. This underscores the significant impact of this parameter on the adsorption process and thus the efficiency of the device. For the analyzed cycle length (300 s), the saturation differences in samples varying in length (B, D, E) are minimal, whereas the differences in the amount of adsorbed vapour are substantial, reaching about 70%. In the analyzed case, designing a longer and thinner bed in the adsorption device would be much more advantageous.

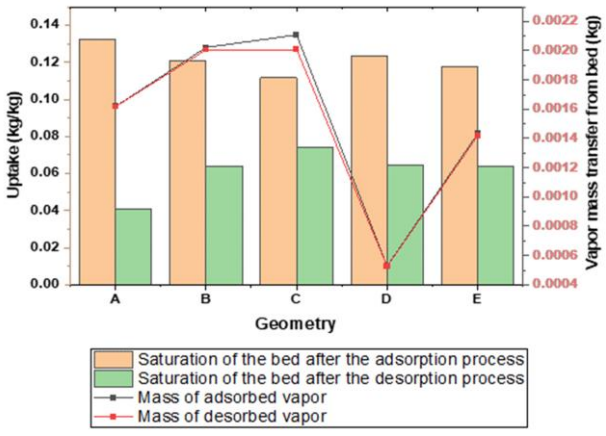

Fig. 17. Summary of water vapor saturation and adsorbed vapor mass for various geometries of the adsorbent bed.

4. Conclusions

The paper presents a method for CFD modelling of the entire adsorption and desorption cycles which enhances understanding of the relationship between these processes and the impact of various factors such as the cycle duration, the temperature of the cooling/heating medium, operating pressure, and the geometry of the sorbent bed on their dynamics. Until now, literature has only modelled either adsorption or desorption processes individually, not the full cycles. This approach allows for the observation of what happens during the transitional period between processes and how this affects their course, which is a novel aspect.

The obtained results demonstrate a significant impact of the adsorbent bed's geometry on the adsorption and desorption processes, emphasizing the crucial role of the distance from the bed centre to the cooling or heating source in the efficiency of these processes. The difference in the amount of vapour adsorbed relative to the amount of sorbent material in beds of different analyzed heights during the adsorption process was 20% higher for the 3 mm bed (A) compared to the 9 mm bed (C). During desorption, the difference in desorbed vapour relative to the amount of sorbent was even greater among these cases of geometry and exceeded 40%. The results indicate that heat exchange significantly influences the progression and control of the adsorption and desorption processes. The length of the bed, affecting the water vapour path to the bed's centre, also impacts these processes, particularly in longer cycles. This discovery highlights the increased resistance caused by water vapour saturation in the sorption bed, which becomes more significant in a more saturated bed, a condition more common in longer cycle durations. These results offer valuable insights for designers of cooling devices based on adsorption technology. Appropriately tailored geometry of the heat exchanger with the sorbent bed can achieve the same effects despite a smaller amount of sorbent, which translates into a smaller device size and cost.

Acknowledgements

The research was conducted within the framework of the "Industrial Doctorate" program by the Ministry of Education and Science (MEiN) titled "Optimization of adsorption and desorption processes in a cooling device using 3D simulations", carried out at the Cracow University of Technology and the company M.A.S. Ltd., under contract number DWD/6/0534/2022.

References

[1] Sztekler, K., Siwek, T., Kalawa, W., Lis, L., Mika L., Radomska E., & Nowak, W. (2021). CFD Analysis of Elements of an Adsorption Chiller with Desalination Function. *Energies*, 14(22), 7804. doi: 10.3390/en14227804

[2] Janusz, S., Szudarek, M., Rudniak, L., & Borcuch, M. (2023). Analysis of heat and mass transfer in an adsorption bed using CFD methods. *Archives of Thermodynamics*, 44(2), 177−194. doi: 10.24425/ather.2023.146564

[3] Manila, M., Mitra, S., & Dutta, P. (2020). Studies on dynamics of two-stage air cooled water/silica gel adsorption system. *Applied Thermal Engineering*, 178, 115552. doi: 10.1016/j.applthermaleng.2020.115552

[4] Li, M., Zhao, Y., Long, R., Liu, Z., & Liu, W. (2022). Computational fluid dynamic study on the adsorption-based desalination and cooling system. *Applied Thermal Engineering*, 508, 115048. doi: 10.1016/j.desal.2021.115048

[5] Gado, M., Ookawara, S., & Hassan, H. (2023). Utilization of triply periodic minimal surfaces for performance enhancement of adsorption cooling systems: Computational fluid dynamics analysis. *Energy Conversion and Management*, 277, 116657. doi: 10.1016/j.enconman.2023.116657

[6] Wang, D., Wu, J., Xia, Z., Zhai, H., Wang, R., & Dou, W. (2005). Study of a novel silica gel–water adsorption chiller. Part II. Experimental study. *International Journal of Refrigeration*, 28(7), 1084−1091. doi: 10.1016/j.ijrefrig.2005.03.002

[7] Petrovic, F., & Mario, K. (2023) Numerical and experimental performance investigation of a heat exchanger designed using topologically optimized fins. *Applied Thermal Engineering*, 218, 119232. doi: 10.1016/j.applthermaleng.2022.119232

[8] Mikhaeil, M., Gaderer, M., & Dawoud B. (2022) Experimental Investigation of the Adsorption and Desorption Kinetics on an Open-Structured Asymmetric Plate Heat Exchanger; Matching Between Small-Scale and Full-Scale Results. *Frontiers in Energy Research*, 10, 818486. doi: 10.3389/fenrg.2022.818486

[9] Critoph, R., & Metcalf, J. (2004). Specific cooling power intensification limits in ammonia–carbon adsorption refrigeration systems. *Applied Thermal Engineering*, 24(5), 661−678. doi: 10.1016/j.applthermaleng.2003.11.004

[10] Gamze, I., Hasan, D., Moghtada, M., & Bidyut, S. (2019). A new adsorbent bed design: Optimization of geometric parameters and metal additive for the performance improvement. *Applied Thermal Engineering*, 162, 114270. doi: 10.1016/j.applthermaleng.2019.114270

[11] Zepeng, W., Yuan, Z., Du, C., Liu, Y., & Wang, J. (2022). Performance of solar adsorption cooling system with internal finned vacuum tube bed. *Case Studies in Thermal Engineering*, 34, 102063. doi: 10.1016/j.csite.2022.102063

[12] Bakhshandeh, M., Zarei, T.Z., & Khorshidi, J. (2022). CFD study on Beds of an Adsorption desalination system in order to improve bed performance. *Chemical Process Design*, 1(2), 60−74. doi: 10.22111/CPD.2023.44116.1015

[13] Boruta, P., Bujok, T., Mika, Ł., & Sztekler, K. (2022). Adsorbents, Working Pairs and Coated Beds for in Adsorption Chillers − State of the Art. *Energies*, 14(15), 4707. doi: 10.3390/en14154707

[14] Li, M., Zhao, Y., & Long, R. (2021). Gradient porosity distribution of adsorbent bed for efficient adsorption cooling. *International Journal of Refrigeration*, 128, 153−162. doi: 10.1016/j.ijrefrig.2021.03.013

[15] Mohammed, H., Mesalhy, O., Elsayed, M., & Chow, L. (2019). Assesment of numerical models in the evaluation of adsorption cooling system performance. *International Journal of Refrigeration*, 99(1), 166−175. doi: 10.1016/j.ijrefrig.2018.12.017